Investigations into Volumetric Stability of Aggregates and Shrinkage of Concrete as a Composite

Shingo Asamoto[1], Tetsuya Ishida[2] and Koichi Maekawa[3]

Abstract

The authors aim to quantitatively understand the influence of various aggregate properties on concrete shrinkage behavior based on both experimental and numerical approaches. The multi-scale constitutive model reveals that differences in aggregate Young's modulus cannot be solely responsible for the observed significant difference in corresponding shrinkage behavior of concrete. Hence, shrinkage of the aggregate itself is considered as a possibility and an aggregate shrinkage model that takes into account the surface area and the degree of aggregate saturation is proposed on the basis of earlier experimental results. The proposed model reasonably simulates the greatly varying different shrinkage behavior of concretes with various types of aggregates.

1. Introduction

It is well known that aggregate properties strongly affect the time-dependent mechanical properties of concrete, such as shrinkage and creep (Troxell *et al*. 1958; Snowdon and Edwards 1962; Hansen and Nielsen 1965; Goto and Fujiwara 1979; Neville 1970, 1995; Arai *et al*. 1999, 2000; Tatematsu *et al*. 2001; Imamoto *et al*. 2006). Recently, it was reported that a prestressed reinforced concrete (PRC) bridge in Japan had suffered severe cracking of RC member surfaces because shrinkage was much greater than predicted at the design stage. In this case, aggregate properties were considered as one of the reasons for the serious damage to the bridge (JSCE concrete committee 2005). Since high-quality aggregate is hardly ever used in practice, it is essential to take into account the influence of various types of aggregate on the mechanical behavior of concrete, including shrinkage and creep, in order to ensure that concrete structures provide the intended performance.

The effect of aggregate properties on concrete shrinkage was comprehensively studied by Goto and Fujiwara (1979). They experimentally investigated the shrinkage behavior of concretes with different aggregates to understand the individual influence of each aggregate property on shrinkage and concluded that shrinkage of the aggregate itself significantly increases concrete shrinkage. They indicated that the role of aggregate in concrete is not only to confine volumetric change; it also contributes to concrete shrinkage by

shrinking itself. Recently, Tatematsu *et al*. (2001) and Imamoto *et al*. (2006) also studied concrete shrinkage from the viewpoint of aggregate properties and reached the same conclusions as Goto and Fujiwara (1979).

On the other hand, concrete shrinkage is also affected by other properties of the aggregate, such as elastic modulus and water absorption. It has been reported that the lower Young's modulus of lightweight aggregate can lead to greater shrinkage in lightweight concrete as compared to that of normal-weight concrete (Neville 1995; JSCE 2002). It is also possible that the abundance of moisture in porous aggregate partially compensates for the drying of concrete pores and reduces shrinkage of lightweight concrete (JSCE 2002). These diverse conclusions can be attributed to coupling of mechanisms relating to various properties of aggregate. It is important to study the contribution of each aggregate property that affects concrete shrinkage and to develop a model that simulates the correlative phenomena comprehensively.

In this paper, the authors aim to quantitatively clarify the contributions of aggregate properties such as water absorption, Young's modulus and aggregate shrinkage to concrete shrinkage based on combined experimental and analytical approaches. The objective is to enhance a multi-scale constitutive model(Maekawa *et al*. 2003; Zhu et al. 2004; Asamoto et al. 2006) by idealizing aggregate properties and behavior appropriately and to evaluate the shrinkage behavior of concrete for any mix proportion under arbitrary environmental conditions.

2. Numerical simulation of concrete shrinkage by the existing model

2.1 General scheme of multi-scale constitutive model
The authors have developed thermodynamics-oriented models for the hydration reaction, pore structure formation, moisture transport/equilibrium and system dynam-

[1]Assistant Professor, Dept. of Civil and Environmental Eng., Saitama University, Japan.
E-mail:asamoto@mtr.civil.saitama-u.ac.jp
[2]Associate Professor, Dept. of Civil Eng., The University of Tokyo, Japan.
[3]Professor, Dept. of Civil Eng., The University of Tokyo, Japan.

ics and brought them together in the computer program known as DuCOM (Maekawa *et al.* 1999). Recently, a project to couple the microscopic thermo-physical information obtained from DuCOM with macroscopic structural information such as stress, strain, deformation, cracking and others as computed by a 3D FEM structural system named COM3 (Maekawa *et al.* 2003) has been in progress. One of the targets of this project is the development of a multi-scale constitutive model that can simulate concrete time-dependent behavior such as shrinkage and creep based on the hydration reaction, pore structure and moisture state in the pores (Maekawa *et al.* 2003; Zhu *et al.* 2004; Asamoto *et al.* 2006). In this section, the multi-scale constitutive model is described in summary. Further details can be found in the literature (Maekawa *et al.* 2003; Zhu *et al.* 2004; Asamoto *et al.* 2006).

In the model, concrete is idealized as a two-phase composite with aggregate and hardening cement paste. The aggregates are modeled as elastic particles with a stiffness determined by their density, while the hardening of cement paste is expressed by the progressive formation of finite fictitious clusters as hydration proceeds based on solidification theory (Bazant and Prasannan 1989). The number of clusters is dependent on the degree of hydration as obtained from DuCOM. The stress in the hardening paste is given as the summation of stresses applied to all clusters. Both volumetric

and deviatoric terms of stress and strain are computed, taking into account interactions between aggregate particles and the cement paste matrix.

According to the model, the mechanical behavior of a fictitious cluster is associated with the thermodynamic state of moisture in micro-pores such as capillary pores, gel pores and interlayer pores. Recently, the authors divided moisture migration in gel pores into moisture transport through the internal pores of CSH gel grains and water in motion within the inter-particle spaces of hydrate micro-products (Asamoto *et al.* 2006). The motion of moisture in capillary and gel pores is idealized based on seepage theory, which describes moisture in pores migrating gradually under sustained stress. The rate of motion depends on pore size, so it takes longer for moisture in smaller pores to reach equilibrium. The moisture in interlayer pores is assumed to disperse only at high temperature and to give rise to the volumetric change due to the dispersion. The deformation of each component is expressed by an elastic spring, a dashpot and a slider whose parameters are determined by hardening cement paste temperature, moisture saturation, pore size distribution and other factors. **Figure 1** represents an overview of the model.

In the model, the authors assume that the driving force behind volumetric change is related to capillary pressure and solid surface energy. These phenomena are computed in consideration of coupling with the ther-
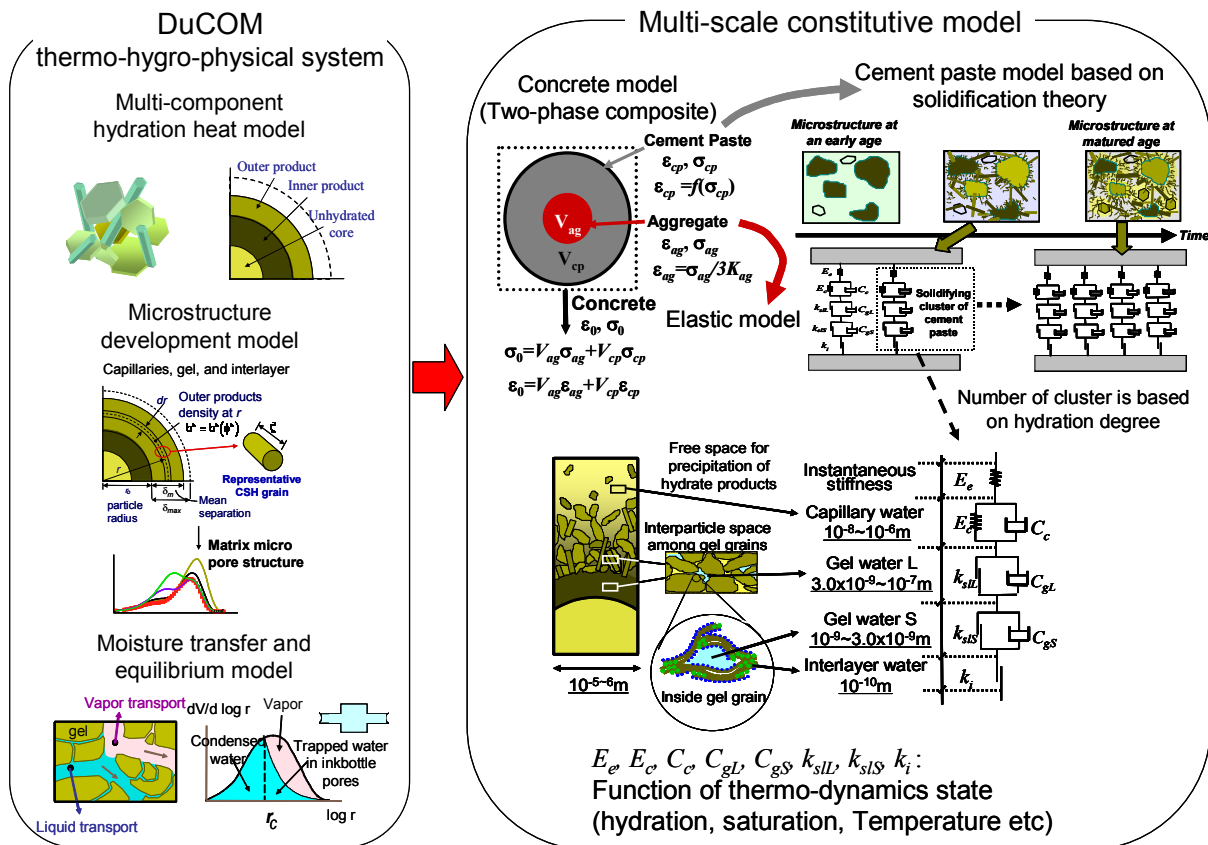
Fig. 1 Schematic representation of multi-scale constitutive model.

modynamic state of moisture in the micro-pores. The capillary force is calculated based on the Laplace equation, the Kelvin equation and the degree of saturation of capillary and gel pores subjected to pore pressure. The shrinkage under relatively high humidity drying conditions is caused mainly by the capillary force in the model. On the other hand, in the case of relatively low humidity conditions, the increase in the solid surface energy of gel particles due to desorption of adsorbed water is idealized as the main mechanism of shrinkage. By coupling the above volumetric stress depending on moisture states in pores with the C-S-H skeleton stress, the equilibrium between skeleton stress and external loading can be satisfied. Thus, time-dependent deformation can be computed according to the boundary conditions without conventional classifications such as autogenous/drying shrinkage and basic/drying creep. Currently, the model is able to reasonably simulate the time-dependent deformation of cementitious composites under arbitrary boundary conditions (Zhu *et al.* 2004; Asamoto *et al.* 2006).

2.2 Verification and sensitivity analysis for shrinkage of concrete with various types of aggregate

The above model is used to study the cause of severe cracking found in the actual structure. The structure in question is a PRC bridge, located in Wakayama Prefecture, central Japan. The bridge had been reported as being seriously damaged. A number of cracks were found on the surface of the RC members and vertical cracks were observed in the web even though it was horizontally prestressed. Only three years had passed after the construction at the time of inspection. The JSCE (Japan Society of Civil Engineers) set up an emergency committee to investigate the reasons for the cracking damage, check the current structural performance of the bridge and determine suitable repair/strengthening measures to be taken. According to the committee, one of the reasons for this serious damage might have been excessive shrinkage of the concrete (JSCE concrete committee 2005). Since such serious concrete shrinkage was thought to be associated with aggregate properties, the committee studied the influence of aggregate properties on concrete shrinkage. Shrinkage experiments using several concretes with different types of aggregates were conducted. **Table 1** shows the mix proportions of these concretes. The aggregates for mix A were from the same source as used for the bridge concrete, while the aggregates for mix B were standard ones extracted from a different site. The sand in mix C was standard but the gravel was the same as that in mix A. The specimen size for autogenous shrinkage and drying shrinkage testing was 10 x 10 x 40 cm. The specimens for autogenous shrinkage testing were sealed immediately after casting and stored at a constant temperature of 20°C. In the case of drying shrinkage tests, specimens were subjected to 60% relative humidity at 20ºC after 7 days of moist

Table 1 Mix proportions in committee test (kg/m^3) (JSCE concrete committee 2005).

	Water	Cement	Sand 1		Sand 2		Gravel	
Mix A	172	453	482	S1	119	S2	1053	G1
Mix B	172	453	544	S3	61	S4	1065	G2
Mix C	172	453					1053	G1

S1, S2: similar sand to that used in PRC bridge concrete
S3, S4: normal sand
G1: similar gravel to that used in PRC bridge concrete
G2: normal gravel

curing.

One of the aggregate properties thought to be possibly responsible for the large shrinkage of the bridge concrete was the relatively lower elastic modulus in comparison with normal aggregate, even though it was not measured (JSCE concrete committee 2005). Thus, the influence of aggregate Young's modulus on concrete shrinkage was examined using our analytical model. In the two-phase composite model, the aggregate Young's modulus is assumed to be the average of the values for sand and gravel. An empirical model of Young's modulus based on the average density of sand and gravel is idealized as (Zhu *et al.* 2004),

$$E_{ag} = (2.35 \cdot \gamma_{ag} - 5.78) \cdot 10^5 \qquad (1)$$
$$\gamma_{ag} > 2.46$$

where, E_{ag} is the average Young's modulus of sand and gravel [MPa] and γ_{ag} is the average density of sand and gravel [g/cm^3].

According to Eq. (1), the aggregate Young's modulus of mix A is computed as 31.6 GPa. In the simulation, a 10% lower value of estimated Young's modulus, 28.4 GPa, was adapted, considering that the aggregates for mix A may be softer than normal as described above. In the case of mix B, the Young's modulus obtained from Eq. (1), 37.8 GPa, was used because the aggregates for mix B are standard ones. In the simulation, the transport of moisture in aggregate pores is taken into account by considering aggregate absorption in the model (Mix A: 1.86%; Mix B: 1.09%). The moisture model for the aggregate will be described in detail in Section 3.

The experimental results and computed results of autogenous shrinkage and drying shrinkage are depicted in **Fig. 2**. In the case of the concrete with the normal aggregate, the model simulates shrinkage reasonably, although the computed results are slightly lower than the observed values. On the other hand, both the observed autogenous shrinkage and drying shrinkage of the mix A concrete containing the same aggregate as the bridge concrete are much larger than those calculated by the model. This significant difference cannot be explained by experimental inaccuracies such as chamber control, or experimental scatter related to the variability of the material properties.
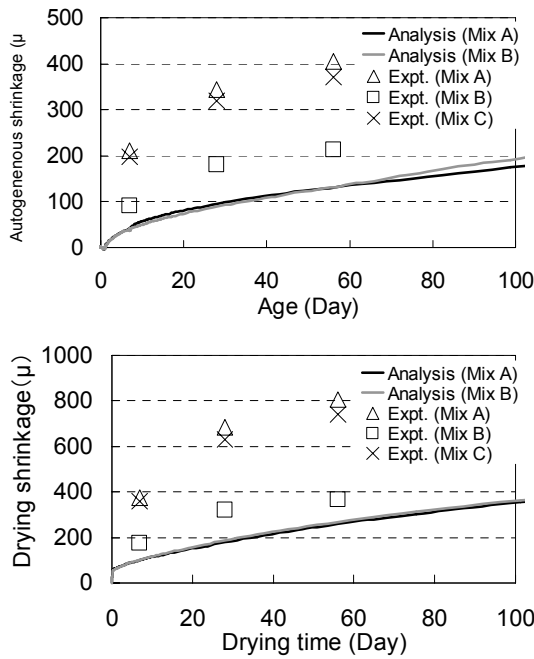
Fig. 2 Computed results and experimental results of autogenous shrinkage and drying shrinkage.

Since the inference of this result is that the 10% reduction in aggregate Young's modulus is insufficient to represent the large concrete shrinkage due to softer aggregate, the stiffness value in the computation was further reduced. As shown in **Fig. 3**, the numerical simulation results almost matched the experiment ones when the aggregate Young's modulus was decreased to 1.0 GPa. Such an extremely low stiffness, however, is only likely to be found in special aggregate such as artificial lightweight aggregate. It is difficult to imagine that the aggregate used in the mix A concrete had such a low stiffness, since it satisfied the physical and chemical properties specified in Japanese industrial standard.

Next, the possibility of low aggregate stiffness is discussed from the aspect of the Young's modulus of concrete. The Young's modulus of typical normal strength concrete in Japan can be estimated by its cylinder compressive strength (Okamura 2000).

$$E_c = 8500 \cdot f_c^{1/3} \qquad (2)$$

where, E_c is Young's modulus of concrete [MPa] and f_c is cylinder compressive strength [MPa]. Since the Young's modulus of the aggregate for mix A was not measured and only the compressive strength was reported(JSCE concrete committee 2005), the approximate estimation is carried out based on the above empirical equation.

Since the compressive strength of the concrete for mix A at 28 days of age is 68.3 MPa, its Young's modulus is computed to be 34.7 GPa given by Eq. (2).

Through the use of the two-phase composite model, the calculated concrete Young's modulus at 28 days of age is 13.5 GPa when the aggregate Young's modulus is set to 1.0 GPa, as shown in **Fig. 4**. Since this concrete Young's modulus is significantly different from the value estimated from the compressive strength, it is very unlikely that the Young's modulus of the aggregate is so low.

As discussed above, the assumption of low aggregate stiffness is not able to offer a consistent explanation of both concrete shrinkage and stiffness. A more detailed investigation of aggregate stiffness is provided in the next section from both experimental and analytical perspectives. The focus is on two points: the validity of the two-phase composite model for simulating concrete
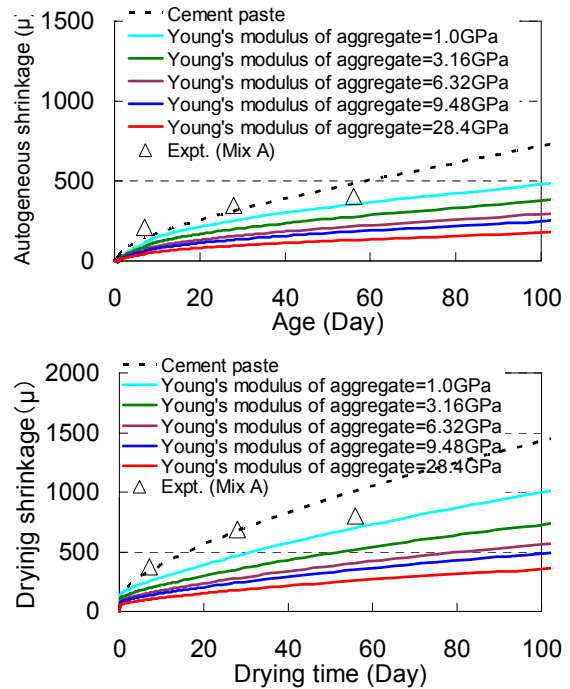
Fig. 3 Computed results of shrinkage with aggregates of varying Young's modulus.
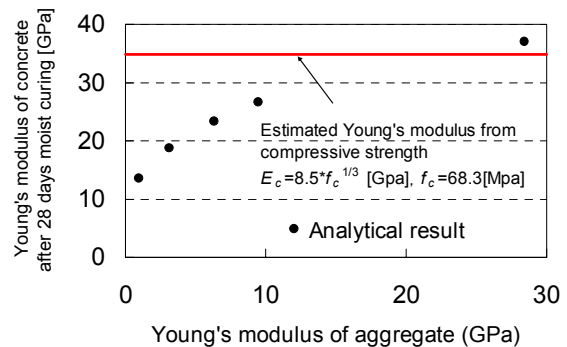
Fig. 4 Computed results of Young's modulus of concrete with aggregates of varying Young's modulus.

behavior in the case of concrete containing soft aggregate and the need to consider other aggregate properties that might lead to increased concrete shrinkage, such as the possibility of aggregate shrinkage that has been pointed out in previous research.

3. Effect of aggregate stiffness and porosity on moisture loss and shrinkage of concrete

3.1 Aggregate properties to affect time-dependent behavior of concrete

The influence of aggregate properties on concrete shrinkage has been a subject of study for decades. It has been reported that the shape, elastic modulus, and water absorption of aggregate, as well as the adherence of clay to its surface and other properties, affect the time-dependent deformation of concrete. The elastic property of aggregate seems to have a particularly large effect on concrete shrinkage and creep because of the restraining effect of the aggregate. The influence of aggregate stiffness on the time-dependent deformation of concrete has been investigated comprehensively by experimental studies on the behavior of concrete containing extremely stiff or soft materials such as steel, glass and rubber in place of normal aggregate (Upendra 1964; Tazawa *et al.* 1992; Ono and Shimomura 2005).

However, since the shape and density of steel, glass and rubber particles are quite different from those of sand and gravel particles, it is not clear that theories derived from shrinkage tests on concretes containing these alternative materials can be applied to concrete with normal aggregate. Further, the effect of moisture transport between aggregate and hardening cement paste on the time-dependent behavior of concrete needs to be given consideration. To fully study the varying shrinkage behavior of concrete with different types of aggregate, it is essential to clarify the influence of each individual aggregate property on concrete shrinkage and to identify the combined effect of all the properties. In this section, moisture loss and shrinkage of concrete with a variety of aggregate computed by the multi-scale constitutive model are compared with experimental results, with the focus on the contribution of aggregate absorption and stiffness, and then the model is verified quantitatively. Throughout this discussion, normal weight aggregate (natural aggregate as used in general-purpose concrete) is defined as normal aggregate (gravel or sand).

3.2 Analytical model for moisture transfer and equilibrium in aggregate pores

In the multi-scale constitutive model, the effect of moisture migration between aggregate and cement paste on concrete behavior as well as aggregate Young's modulus can be taken into account by considering the average properties of sand and gravel, including density, particle size, volume ratio and absorption. In this section,

the model for representing the moisture transfer and equilibrium in aggregate pores is summarized and compared with previous experimental study on moisture loss of concrete containing lightweight aggregate.

Moisture transport between aggregate and cement paste is idealized in DuCOM as follows (Maekawa *et al.* 1999),

$$R_{paste,ag} = \alpha_{paste,ag}(P_{ag} - P_{paste}) \tag{3}$$

where, $R_{paste,ag}$ is the moisture exchange rate from cement paste to aggregate [Pa/m.s], $\alpha_{paste,ag}$ is the local mass transfer coefficient between cement paste and aggregate [1/m.s], P_{ag} is the aggregate pore pressure [Pa] and P_{paste} is the cement paste pore pressure [Pa].

According to DuCOM, $\alpha_{paste,ag}$ is given by assuming that the aggregate consists of spheres of the same radius,

$$\alpha_{paste,ag} = \frac{3\beta G}{r_{ag}^2}\left(\frac{1}{2K_{ag}} + \frac{(G_0/G)^{1/3}-1}{K_{paste}}\right)^{-1} \tag{4}$$

where β is the apparent effectiveness of moisture transfer across the actual area of contact, G is the volumetric concentration of aggregate [m³/m³], G_0 is the limit filling capacity of aggregate [m³/m³], r_{ag} is the average aggregate radius [m], K_{ag} is the permeability of aggregate pores [m/s] and K_{paste} is the permeability of cement paste [m/s].

Here, β denotes a parameter representing the apparent effectiveness of moisture transfer across the contact areas between the paste and aggregate. When moisture migration between cement paste and aggregate is ideal, β becomes 1.0, while it is 0.0 when there is no moisture transport from or into the aggregate. Using the approximation that $K_{paste} \ll K_{ag}$, $\alpha_{paste,ag}$ is given as,

$$\alpha_{paste,ag} = \frac{3\beta G K_{paste}}{r_{ag}^2\left\{(G_0/G)^{1/3}-1\right\}} \tag{5}$$

In order to determine unknown parameter β, parametric studies were conducted using the above moisture transport model between cement paste and aggregate. Since the sensitivity of parameter β has not been clearly investigated yet, in this analysis, the authors tried to identify an approximate value of β by matching to experimental data of a previous study (Kokubu *et al.* 1969).

Moisture migration in aggregate pores depends on the aggregate isotherm that represents the relationship between pore humidity and moisture saturation. Here, the isotherm of normal aggregate proposed by Nakarai and Ishida (2003) based on experiments with normal sand was adapted. In the case of concrete with normal sand and lightweight gravel, it is supposed that the lightweight gravel is almost fully dried of moisture at relatively high levels of humidity due to the large pores so the average saturation of the aggregate depends on the sand saturation at relatively lower humidity levels. The

proposed isotherm is shown in **Fig. 5**.

The experimental conditions adopted in the investigation of parameter β are summarized in **Table 2** (Kokubu *et al*. 1969). The parametric numerical results of moisture loss obtained by varying parameter β are shown in **Fig. 6**. With a larger value of β, the model is able to simulate moisture loss at the beginning of drying more reasonably, even though it is a slight improvement. **Figure 7** shows the variations in cement paste and aggregate pore humidity in the model for cases where β is more than 0.01. When β is more than 0.1, moisture moves rapidly between cement paste and aggregate and the pore humidity of the cement paste almost corresponds to that of the aggregate during drying. Currently, the authors do not have a clear microscopic understanding of the possibility of this phenomenon under actual
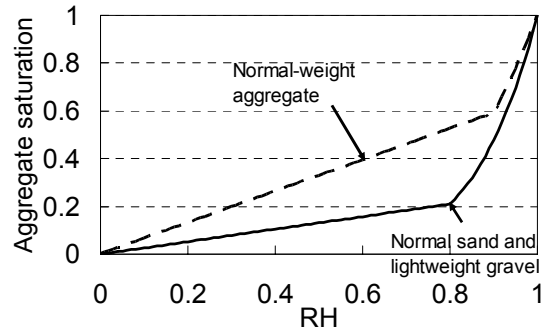
Fig. 5 Isotherm between pore humidity and aggregate saturation (Nakarai and Ishida 2003).

Table 2 Mix proportion of lightweight concrete and normal weight concrete and experimental outline (Kokubu *et al*. 1969).

Specimen	Unit water content (kg/m^3)	Sand			Gravel		
		Type	Absorption (%)	Density (g/cm^3)	Type	Absorption (%)	Density (g/cm^3)
NN	158	River sand (N)	1.9	2.63	River gravel (N)	1.1	2.66
ON	159	River sand (N)	1.9	2.63	Artificial lightweight gravel (O)	10.5	1.50
XN	162	River sand (N)	1.9	2.63	Artificial lightweight gravel (X)	16.1	1.46

Water-cement ratio: 0.45; sand volume ratio: 0.4

Specimen size: 10 x 10 x 42 cm prism

Drying conditions: specimen exposed to RH=60% at 21°C after 7 days of moist curing
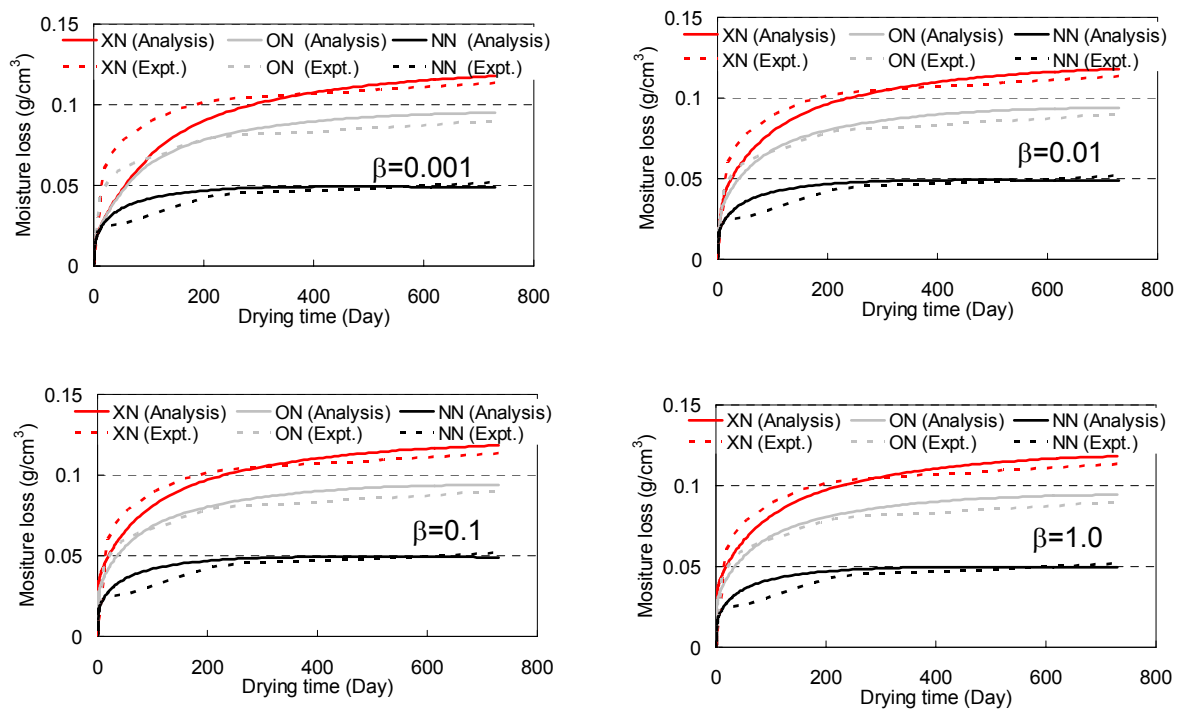
Fig. 6 Parametric study of parameter β.
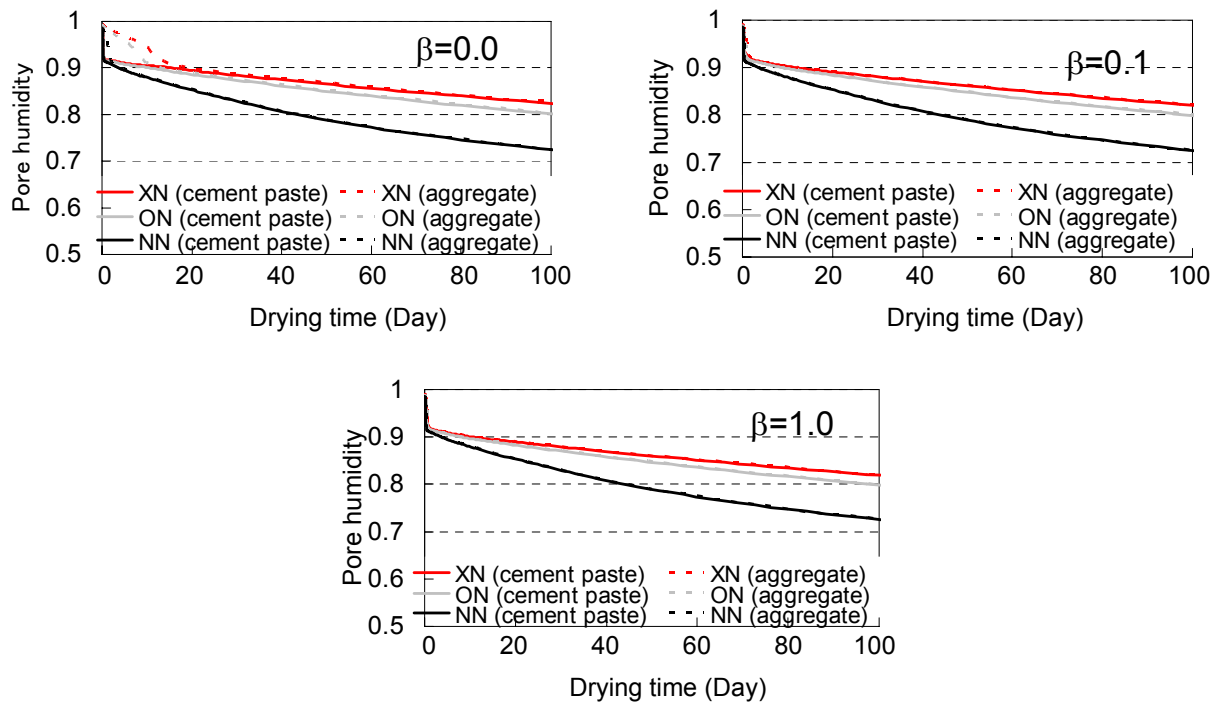
Fig. 7 Pore humidity with varying parameter β.

drying conditions. Thus, β was specified simply as 1.0 because the computed results with this value for moisture loss have better agreement with experiment.

3.3 Summary of experimental program

The experimental results shown in **Fig. 2** suggest that gravel properties can significantly affect concrete shrinkage, since the different gravel types in specimens of mix B and of mix C lead to a large difference in shrinkage, while the shrinkage of the mix A and mix C specimens made with the same gravel but different sands is small. Given these results, the shrinkage behavior of concretes made with different gravels (normal weight aggregate and artificial lightweight aggregate) was studied for the purpose of examining the effect of stiffness and water migration. The lightweight gravel had significantly lower Young's modulus and higher water absorption than the normal gravel.

The material properties of the normal aggregate and lightweight aggregate used in the test are shown in **Table 3**. The lightweight gravel coated with epoxy resin on the surface was also used in one of the test sets in order to prevent moisture migration from the gravel. **Table 4** represents the mix proportions used in this experimental program. The type of sand and the volume ratio of aggregate were the same in every mix proportion. The specimens cast using normal gravel are referred to as **OG** (**O**rdinary **G**ravel), the ones containing lightweight gravel are named **LG** (**L**ightweight **G**ravel) and specimens with epoxy-coated lightweight gravel are identified as **ELG** (**E**poxy-coated **L**ightweight **G**ravel). For ex-

Table 3 Aggregate properties.

	Density (g/cm^3)*	Absorption (%)
Sand (crushed sandstone)	2.59	1.55
Gravel (crushed sandstone)	2.66	0.45
Artificial lightweight gravel	0.45	27.5

(*) Density of artificial lightweight gravel is in oven-dry condition. Density of other aggregates is in saturated surface-dry condition.

Table 4 Mix proportion (kg/m^3).

Specimen	W/C	Water	Cement	Sand	Gravel	SP
OG30	30	160	533	686	1039	3.73
LG30	30	160	533	686	176	3.73
OG50	50	201	403	686	1039	-
LG50	50	201	403	686	176	-

Mix proportions of specimens ELG30 and ELG50 are the same as specimens LG30 and LG50, respectively.

ample, OG30 stands for a specimen with W/C=30% made with normal aggregate. In the case of low water-cement ratio, a superplasticizer was added to avoid the problem of insufficient compaction. The lightweight gravel for LG specimens was submerged in water and then used in saturated surface-dry condition, while the gravel surface for ELG specimens was manually ep-

oxy-coated after oven-drying. Photo in **Fig. 8** shows the epoxy-coated gravel used in the ELG specimens. When prepared epoxy-coated gravel was immersed in water, the weight increase was limited to around 3% in spite of the high absorption of the uncoated gravel (27.5%). This test demonstrates that epoxy coating is an effective way of preventing moisture migration into the gravel. The gravel for ELG specimens was mixed manually to avoid damaging the epoxy-coated surface, while OG and LG concretes were mixed in a twin shaft mixer. In order to exclude the influence of these different mixing methods on shrinkage behavior, the mortar for ELG specimens was first mixed in the twin shaft mixer and then the gravel was manually distributed in the mortar.

Prismatic specimens measuring 10 x 10 x 40 cm were used in the experiment. The form was removed one day after casting and then the specimens were cured in water at 20±2°C for six days. After this period of moist-curing, specimens were exposed to 60±5% relative humidity at 20±2°C. Strains were measured with contact gauges having 5µ resolution. All the results in drying shrinkage tests were obtained from the average of two specimens per each experimental condition.

The objective of the experiment was to evaluate the influence of aggregate stiffness on concrete shrinkage while eliminating variations in pore humidity and aggregate shrinkage by epoxy coating the lightweight aggregate. It was expected that the epoxy coating would prevent moisture transport between aggregate and hardening cement paste while maintaining the same gravel stiffness. It was, however, necessary to investigate whether the epoxy-coated interface between gravel and cement paste affects shrinkage behavior. To study the effect of the epoxy coating, shrinkage tests were conducted using normal gravel and epoxy-coated normal gravel. The influence of the epoxy interface on shrinkage was directly examined in this test because there is very little water migration with non-epoxy-coated normal gravel due to its low water absorption, as shown in **Table 3**.

In the test, a specimen with a mix proportion of OG30 was used, since the influence on autogenous shrinkage can also be investigated with a low water-cement ratio. Cylindrical specimens measuring φ10 x 20 cm were sealed after casting and autogenous shrinkage was measured at 20±2°C until 14 days of age. After 14 days, the surface sealing was removed and the specimens were dried at 60±5% relative humidity and 20±2°C. Strain was measured using a mold gauge. **Figure 8** shows the results. The difference between the specimen with normal gravel and the specimen made with epoxy-coated normal gravel in autogenous shrink-

Epoxy-coated artificial lightweight gravel
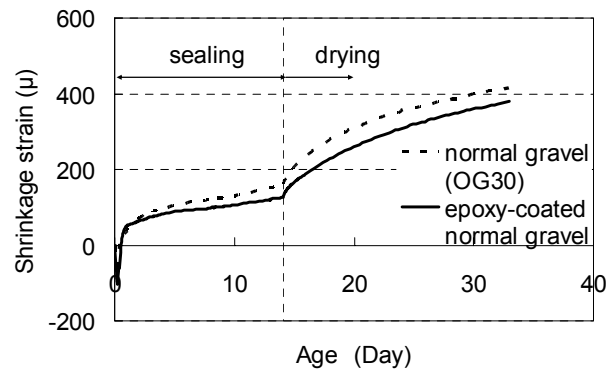
Fig. 8 Experimental study of the influence of epoxy-coated interface between cement paste and gravel on shrinkage.

age was around 30µ at 14 days of age. Even after being subjected to drying conditions, this difference increased by just 5µ (for a total shrinkage differential of around 35µ). According to this experimental result, the epoxy coating on the gravel surface has no significant effect on concrete shrinkage.

The compressive strength and Young's modulus of each specimen at 7 days of age are shown in **Table 5**. The mechanical properties of specimens ELG and LG were rather similar. The test results indicate that the epoxy coating on the gravel surface does not significantly affect bonding between gravel and hardened cement paste. It is concluded that coating the gravel surface with epoxy resin is an effective method of eliminating moisture migration in the gravel, yet maintaining other gravel properties such as stiffness and bonding with the cement paste.

3.4 Influence of aggregate properties on concrete shrinkage

Figures 9 and **10** show the computed results and experimental results for drying shrinkage of concretes with different aggregates. In the simulation, the absorption of epoxy-coated gravel was assumed to be 0.0%, while the absorption values shown in **Table 3** were in-

Table 5 Results of compressive test at 7 days of age.

	OG30	LG30	ELG30	OG50	LG50	ELG50
Compressive strength (MPa)	62.8	18.8	18.1	23.7	7.5	12.9
Young's modulus (GPa)	34.3	14.0	15.5	23.4	9.6	8.8
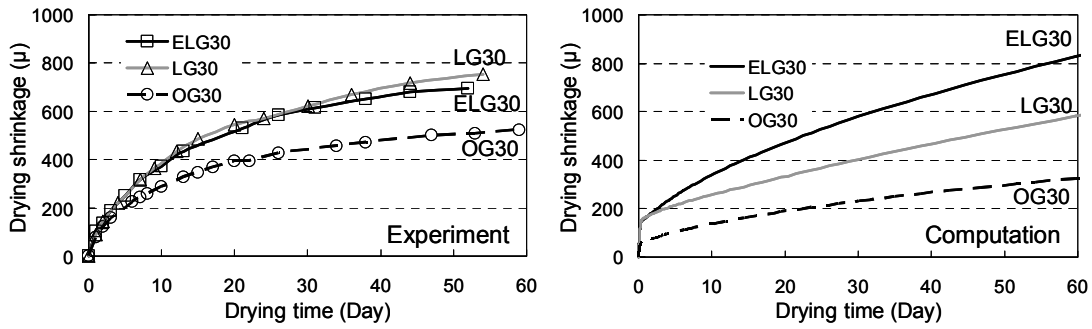
Fig. 9 Experimental results and computed results of drying shrinkage (W/C=30%).
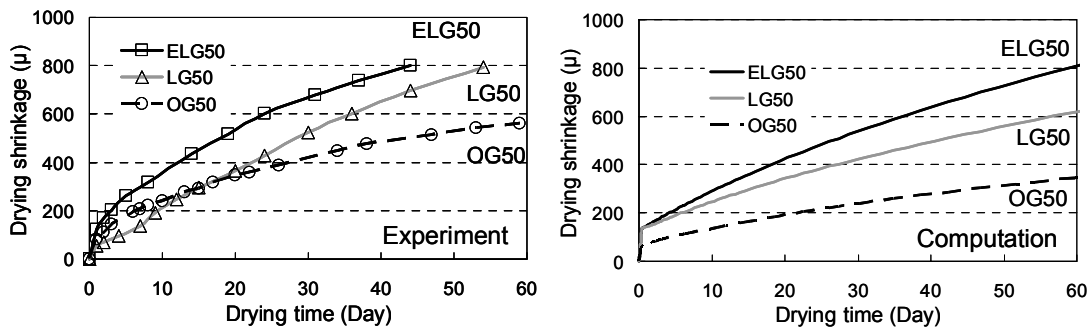
Fig. 10 Experimental results and computed results of drying shrinkage (W/C=50%).

put for the case of other aggregates. As explained in Section 2, the Young's modulus of the aggregate is idealized as an average value of density for sand and gravel. In the case of OG specimens, the Young's modulus of the aggregate is computed to be 40.8 GPa from Eq. (1). Since the average density of the sand and lightweight gravel for LG and ELG specimens is out of range for Eq. (1), the Young's modulus of the aggregate was determined to be 2.0 GPa based on experimental values of concrete Young's modulus. The Young's modulus of hardening cement paste is calculated according to the water-cement ratio and degree of hydration(Zhu *et al*. 2004). **Figure 11** shows the experimental results and computed results for concrete Young's modulus. The two-phase composite model is able to simulate the different elastic stiffnesses of concretes with different aggregate elasticities reasonably well for both low and high water-cement ratios.

Firstly, the influence of moisture in gravel pores on concrete shrinkage is discussed. The water in the gravel pores of LG specimens is gradually transferred into the cement paste matrix and then diffused outside. Since the pore humidity in the concrete of LG specimens is larger than that of ELG specimens due to the diffusion of moisture from the gravel into cement paste at the beginning of drying, the drying shrinkage of LG specimens should be smaller than that of ELG specimens. In the case of high water-cement ratios, this speculation can be verified because both the computed result and the experimental result indicate larger shrinkage of ELG

specimens than LG specimens. On the other hand, for low water-cement ratios, the experiment and analysis give different results. In the numerical simulation, moisture from the aggregate takes a longer time to migrate to the outside through the cement paste matrix due to the dense pore distribution in comparison with high water-cement ratios. Since moisture supplied from porous aggregate remains in the paste matrix and therefore maintains pore humidity, the difference in shrinkage between LG specimens and ELG specimens with low water-cement ratios is larger than that at high water-cement ratios in the calculation. In the experiment, however, moisture in the gravel pores has little effect on shrinkage behavior. One possible reason for the differ-
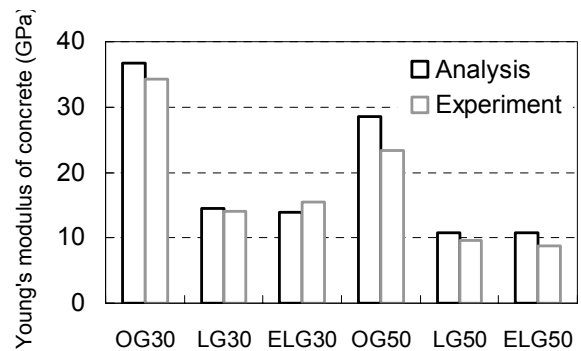
Fig. 11 Young's modulus of each concrete at 7 days of age.

ence is that, in the experiment, moisture from the porous gravel diffuses into the cement paste due to self-desiccation during curing and then may not migrate at drying. Since this assumption has not been verified yet, the authors recognize that further investigation is necessary.

Next, the influence of aggregate Young's modulus on drying shrinkage is investigated. The shrinkage of OG specimens made with stiff normal gravel is compared with that of ELG specimens containing soft epoxy-coated gravel assuming, as noted previously, that moisture in the normal gravel does not affect drying shrinkage due to its low absorption. In the experiment, the shrinkage of ELG specimens with softer gravel is larger than that of OG specimens. The computed result shows the same tendency, so it is concluded that the effect of aggregate stiffness on shrinkage of concrete can be simulated reasonably. In the case of epoxy-coated porous lightweight aggregate with a significantly low elastic modulus, the influence of aggregate stiffness on concrete shrinkage can be exactly observed in the experiment and simulation because moisture migration from aggregate is quite small.

The computed results for the shrinkage of OG specimens are smaller than experimental ones. This appears to be attributed to the aggregate shrinkage of crushed sandstone used in OG specimens, which is discussed in next section.

4. Numerical analysis considering aggregate shrinkage

Based on the discussion given in the previous section, it is inferred that the multi-scale constitutive model is able to simulate the influence of aggregate elastic modulus and water absorption on concrete shrinkage appropriately. Thus, it is suggested that the large concrete shrinkage in the PRC bridge mentioned in Section 2 may be caused not by the low Young's modulus of the aggregate but by other aggregate properties.

It has been reported that aggregate shrinkage as well as elastic modulus may influence the volumetric change of concrete (Snowdon and Edwards 1962; Hansen and Nielsen 1965; Goto and Fujiwara 1979, Tatematsu *et al.* 2001, Imamoto *et al.* 2006). In this section, an aggregate shrinkage model is proposed and implemented in the multi-scale constitutive model. The proposed model is then verified by comparison with experimental results.

The volumetric stresses and strains for a two-phase system are given with respect to the component values as follows,

$$\sigma_0 = V_{cp}\sigma_{cp} + V_{ag}\sigma_{ag} \tag{6}$$

$$\varepsilon_0 = V_{cp}\varepsilon_{cp} + V_{ag}\varepsilon_{ag} \tag{7}$$

$$\varepsilon_{ag} = \frac{1}{3K_{ag}}\sigma_{ag} \tag{8}$$

$$\varepsilon_{cp} = f(\sigma_{cp}) \tag{9}$$

where, σ_0, σ_{cp} and σ_{ag} are the mean volumetric stresses of the concrete, cement paste and aggregate, respectively, and ε_0, ε_{cp} and ε_{ag} are the mean volumetric strains of the concrete, cement paste and aggregate, respectively. V_{ag} and V_{cp} are the volume fractions of aggregate and cement paste, respectively. K_{ag} is volumetric stiffness of aggregate. The aggregate is modeled as perfectly elastic material, while the cement paste is idealized as solidifying material increasing the fictitious clusters due to the progress of hydration, as shown in **Fig. 1**. In addition, the following restrain condition related to shear stiffness of cement paste is assumed,

$$\left(\frac{\sigma_{ag} - \sigma_{cp}}{g(G_{cp})}\right) + (\varepsilon_{ag} - \varepsilon_{cp}) = 0 \tag{10}$$

The function $g(G_{cp})$ is the shear stiffness of cement paste. $g(G_{cp})=4G_{cp}$, which Benveniste (1987) proposed, is used in the model. More detailed information about the interaction between cement paste and aggregate, especially shear deformation and Poisson ratio, can be found in the literature(Zhu *et al.* 2004).

For the purpose of considering aggregate shrinkage due to drying, the shrinkage strain is added to the volumetric strain of the aggregate arising from the volumetric stress as follows:

$$\varepsilon_{ag} = \frac{1}{3K_{ag}}\sigma_{ag} + \varepsilon_{ag}^{sh} \tag{11}$$

where, ε_{ag}^{sh} is the strain of the aggregate due to its shrinkage mechanism.

The drying shrinkage of aggregate is likely to be dependent on moisture states in the aggregate pores based on mechanisms such as capillary pressure and also on the increase in solid surface energy as well as in the concrete. Goto and Fujiwara (1979) presented the relationship between moisture content and shrinkage of normal aggregate for a situation where aggregate absorbed moisture after oven-drying and then dried again, as given in **Fig. 12**. **Figure 13** shows the relationship between the ratio of ε_{ag}^{sh} (drying shrinkage of aggregate) to $\varepsilon_{ag\max}^{sh}$ (maximum shrinkage of aggregate after oven-drying) and degree of saturation S_{ag} (= moisture content/maximum moisture content) obtained from the above experiment by Goto and Fujiwara. Even for different types of aggregate with distinct values of maximum shrinkage strain, the relationship is almost linear through both the drying and wetting processes. Currently, there is no valid experimental evidence that verifies or contradicts this relationship based on a microscopic approach using capillary pressure, solid surface energy or similar. Once the implementation of simple aggregate shrinkage model according to the experimental results and the respective investigation of each aggregate property are noted here, the shrinkage of normal aggregate is idealized as,
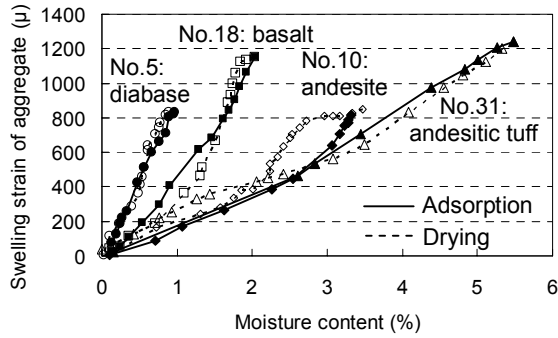
Fig. 12 Length change of normal aggregates due to absorption and drying (Goto and Fujiwara 1979).
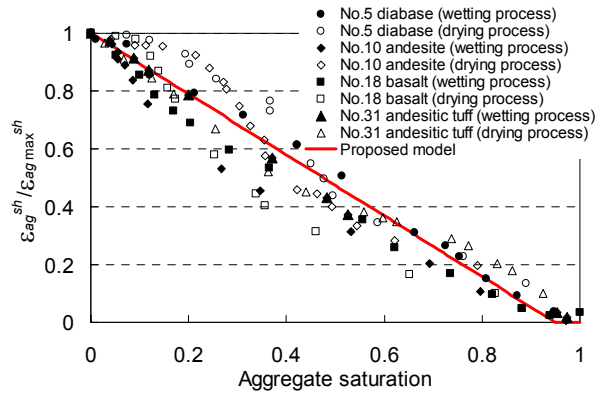
Fig. 13 Relationship between $\varepsilon_{ag}^{sh}/\varepsilon_{agmax}^{sh}$ and aggregate saturation based on Goto and Fujiwara experiment.
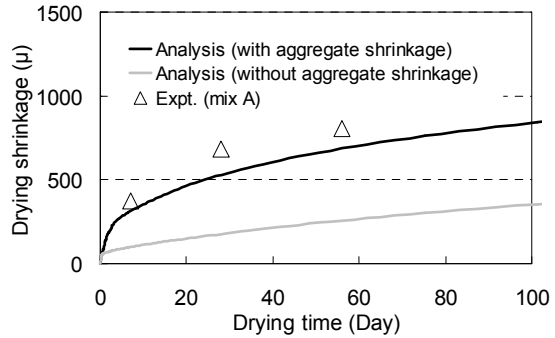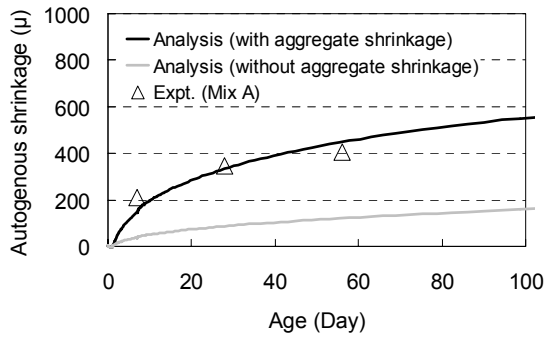
Fig. 14 Computed results considering aggregate shrinkage.

$$\begin{aligned} \varepsilon_{ag}^{sh} &= \varepsilon_{ag\max}^{sh} \cdot (1.0 - S_{ag}/0.95) & S_{ag} &\leq 0.95 \\ \varepsilon_{ag}^{sh} &= 0.0 & S_{ag} &> 0.95 \end{aligned} \qquad (12)$$

The degree of saturation S_{ag} can be computed in the model from the pore humidity as obtained using the moisture transport model and the isotherm, as discussed in previous section. Shrinkage up to a saturation of 0.95 is assumed to be 0μ because the moisture in large pores diffuses first and shrinkage due to changes in pore pressure and solid surface energy related to moisture states in large pores will be small.

The shrinkage of the PRC bridge concrete as discussed in Section 2 is simulated once again using the proposed aggregate shrinkage model. The isotherm between pore humidity and the degree of saturation of aggregate was that proposed by Nakarai and Ishida (2003), as shown in **Fig. 5**. The maximum drying shrinkage ε_{agmax}^{sh} is likely to be extremely large so it was set at 1400μ, the largest value of maximum shrinkage reported in previous research (Goto and Fujiwara 1979). The average elastic modulus of the sand and gravel was assumed to have the value of 28.4 GPa.

Figure 14 shows the computed results of autogenous shrinkage and drying shrinkage and **Fig. 15** gives the calculated aggregate shrinkage strain under sealed and drying conditions. Both autogenous shrinkage and drying shrinkage are significantly larger when simulated in consideration of aggregate shrinkage and the computed results appear reasonable. Further, there is a remarkable amount of aggregate shrinkage 600μ under drying condition, while aggregate also shrinks even under sealed condition due to the self-desiccation of cement paste. These analytical results strongly suggest that the contribution of aggregate shrinkage to concrete shrinkage is considerable and that significantly greater autogenous shrinkage and drying shrinkage can result from aggregate properties alone. Since various types of aggregate are used in cementitious composite materials, it is important to gain a correct understanding of the shrinkage properties of each aggregate during the design process. The model proposed here is further investigated by comparing the computed results with observed shrinkage of concretes made with various aggregates.

In order to evaluate the shrinkage of the aggregate itself, some researchers have focused on the specific surface area of the aggregate. Imamoto *et al*. (2006) reported that the amount of drying shrinkage of concrete is strongly related to the specific surface area of the sand and gravel. Goto and Fujiwara (1979) proposed the following equation associating maximum aggregate
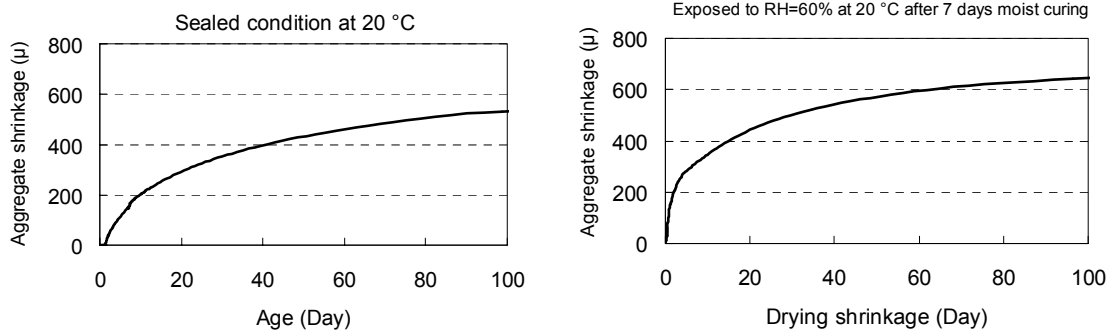
Fig. 15 Aggregate shrinkage in sealed condition and drying condition.

shrinkage strain $\varepsilon_{ag\max}^{sh}$ with specific aggregate surface area $SA_{ag,}$ assuming that the main mechanism of aggregate shrinkage is an increase in solid surface energy due to desorption of adsorbed water.

$$\varepsilon_{ag\max}^{sh} = k \cdot SA_{ag} \qquad (k:\text{constant}) \qquad (13)$$

As shown in **Fig. 16**, an almost linear relationship is obtained experimentally between maximum aggregate shrinkage with oven drying and specific surface area. Since the value of k was not reported in the paper (Goto and Fujiwara 1979), k was determined to be 136 x 10^{-6} by the method of least squares. According to Eqs. (11), (12) and (13), aggregate shrinkage can be computed in the model if the specific surface area of the aggregate is known.

Using the above methodology, computed results were compared with the shrinkage tests carried out by Imamoto *et al.* (2006). The mix proportions of concretes used in the experiments are shown in **Table 6**. The specimen size was 10 x 10 x 40 cm and the specimens were exposed to RH=60% at 20°C after 7 days of moist curing at 20°C. From the specific surface area of aggregate given by Imamoto *et al.* as shown in **Fig. 17**, the maximum aggregate shrinkage was simply determined using Eq. (13) though the method to measure the surface area is different from that in Goto and Fujiwara's experiment: the maximum shrinkage for specimens UT-KT, UK-STo, H2 and L2 was 1021μ, 805μ, 624μ and 387μ, respectively. The Young's modulus of the aggregate used in specimens UT-KT, UK-STo, H2 and L2 was 33.1 GPa, 37.2 GPa, 25.1 GPa and 37.0 GPa, respectively based on Eq. (1).

Figure 18 shows the experimental results and the computed results with and without consideration of aggregate shrinkage. When aggregate shrinkage is included in the analytical model, the varying concrete shrinkage behavior for various types of aggregate is modeled more reasonably than when aggregate shrinkage is ignored. It is concluded, therefore, that the multi-scale constitutive model is able to predict the greatly varying shrinkage of concrete containing a variety of aggregate in consideration of aggregate shrinkage.
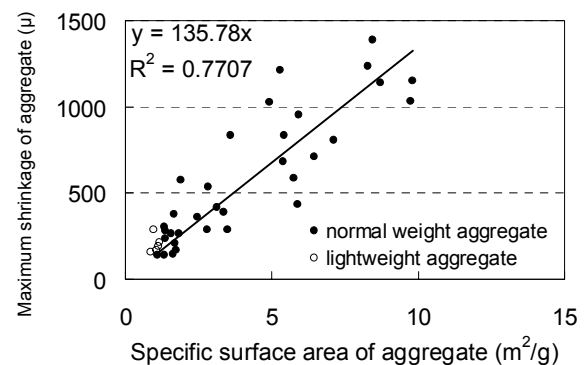
Fig. 16 Relationship between specific surface are and maximum shrinkage of aggregate (Goto and Fujiwara 1979)

Table 6 Concrete mix proportions (kg/m^3) (Imamoto *et al.* 2006)

specimen	W	C	S1	S2	G
UT-KT	180	360	517	222	1006
UK-STo	180	360	522	224	1006
H2	180	360	517	222	980
L2	180	360	517	222	1010

S1(UT-KT, H2, L2): sea sand; density 2.48g/cm^3; absorption 2.50%
S1(UK-Sto): sea sand; density 2.55g/cm^3; absorption 1.61%
S2(UT-KT, H2, L2): hardened sandstone sand; density 2.61g/cm^3; absorption 1.73%
S2(UK-Sto): limestone sand; density 2.58g/cm^3; absorption 1.98%
G(UT-KT, UK-STo): hard sandstone gravel; density 2.66g/cm^3; absorption 0.95%
G(H2): hardened sandstone gravel; density 2.60g/cm^3; absorption 0.73%
G(L2): limestone gavel; density 2.69g/cm^3; absorption 0.41%

5. Conclusion

In this paper, the influence of aggregate properties on concrete shrinkage was studied using both experimental and numerical approaches in order to clarify quantitatively the contribution of each aggregate property to
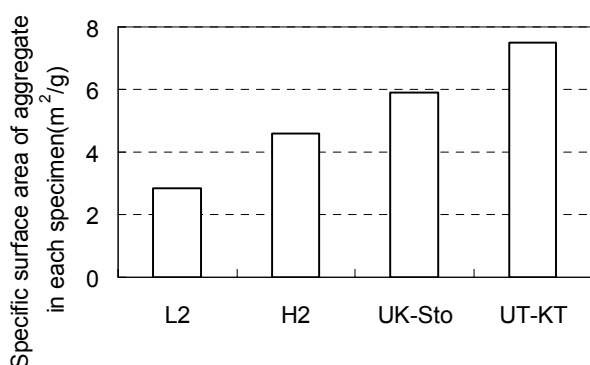
Fig. 17 Specific surface area of aggregate (Imamoto *et al*. 2006).
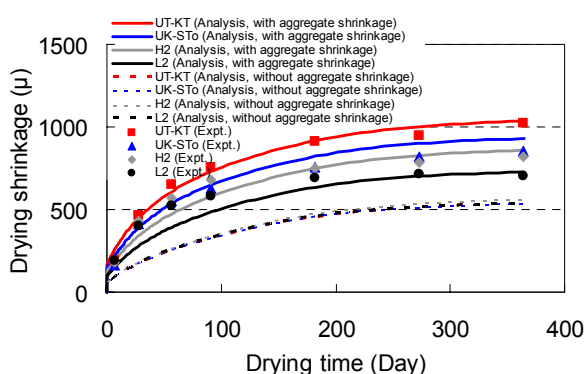
Fig. 18 Computed results of drying shrinkage considering aggregate shrinkage (Experimental data: Imamoto *et al*. 2006).

concrete shrinkage. The results obtained are summarized below.

The sensitivity analysis of concrete shrinkage by varying aggregate Young's modulus indicated that it is not possible to explain the significant increase in concrete shrinkage observed with specific aggregate only in terms of the low elastic modulus of the aggregate. To verify the shrinkage simulation of concrete with soft aggregate, the numerical results were compared with the results of shrinkage tests on concretes made with various aggregates considering Young's modulus and water absorption of aggregate. Concrete containing soft epoxy-coated lightweight gravel exhibited greater shrinkage than that of concrete made with stiffer normal-weight gravel in the experiment. The numerical model provided a reasonable simulation of the different shrinkage behavior of concretes containing these soft and stiff aggregates. Further, the moisture loss and shrinkage of concrete containing porous lightweight aggregate containing significant moisture in its pores was computed acceptably. According to these investigations, it was found that aggregate properties other than low stiffness can have a significant influence on concrete shrinkage.

Based on earlier pioneering research, an aggregate

shrinkage model was proposed and implemented in the multi-scale constitutive model in order to analytically examine the influence of aggregate shrinkage on concrete shrinkage. This demonstrated that the significant increase in concrete shrinkage mentioned above can be calculated when aggregate shrinkage related to aggregate moisture states is taken into account.

Little attention has been paid to the characteristics of aggregate itself, although the design process incorporates consideration of concrete mix proportion, structure size and boundary conditions. The multi-scale constitutive model developed in this work enables the simulation of moisture transport between aggregate and cement paste, as well as the stiffness and shrinkage of hardening cement paste and aggregate, under arbitrary boundary conditions. As a result, the effects of each aggregate property on concrete shrinkage can be determined. According to the analytical work, aggregate properties, especially its shrinkage, are likely to cause the remarkable variation in concrete shrinkage. Since various types of aggregate are generally used in concrete mixes due to the depletion of aggregate such as river aggregate, it is essential to take into account not only aggregate density, absorption and the alkali-silica reaction but also aggregate shrinkage in the design of concrete structures.

References
Arai, M., Tamura, H., Sekiguchi, K., Umeda, H., Iwashimizu, T., Tatematsu, K., Ohashi, M., Urano, H., Kimura, Y., Akashi, T., Motoki, R., Yamasaki, J., Sotoya, Y., Imamoto, K., Annoura, T., Tohyama, S. and Fujisawa, I. (1999). (2000). "Study on influence of aggregate quality on drying shrinkage of concrete (Parts 1-8)." *Summaries of Technical Papers of Annual Meeting*, Architectural Institute of Japan, A-1 (materials and constructions), 741-746 (1999), 645-654 (2000). (in Japanese)

Asamoto, S., Ishida, T. and Maekawa, K. (2006). "Time-Dependent Constitutive Model of Solidifying Concrete Based on Thermodynamic State of Moisture in Fine Pores." *Journal of Advanced Concrete Technology*, 4(2), 301-323.

Bazant, Z. P. and Prasannan, S. (1989). "Solidification theory for concrete creep. I. Formulation, II. Verification and application." *Journal of Engineering Mechanics,* 115(8), 1691-1725.

Benveniste, Y. (1987). "A new approach to the application of Mori-Tanaka's theory in composite materials." *Mechanics of Materials*, 6, 147-157.

Goto, Y. and Fujiwara, T. (1979). "Effect of aggregate on drying shrinkage of concrete." *proceedings of JSCE*, 286, 125-137. (in Japanese); related publication, Fujiwara, T. (1984). "Change in Length of Aggregate Due to Drying." *Bulletin of the International Association of Engineering Geology*, 30, 225-227.

Hansen, T. and Nielsen, K. (1965). "Influence of aggregate properties on concrete shrinkage." *Journal of the American Concrete Institute*, 62(7), 783-794.

Imamoto, K., Ishii, S. and Arai, M. (2006). "Drying shrinkage properties of concretes with several kinds of aggregate and the influence of specific surface areas of the aggregates." *Journal of Structural and Construction Engineering*, Architectural Institute of Japan, 606, 9-14. (in Japanese); related publication, Imamoto, K. and Arai, M. (2005). "The influence of specific surface area of coarse aggregate on drying shrinkage of concrete." *Creep and Shrinkage and Durability Mechanics of Concrete and Other Quasi-brittle Materials (Concreep.7)* Nantes, France, 95-100.

JSCE Guidelines for Concrete No. 3 Standard Specifications for Concrete Structures – 2002 (2002). "Structural Performance Verification."

JSCE concrete committee (2005). "Interim report on deterioration of Tarui bridge." (in Japanese)

Kokubu, M., Kobayashi, M., Okamura, H. and Yamamoto, Y. (1969). "Problems of lightweight aggregate concrete." *Concrete Library of JSCE*, 24, 1-13. (in Japanese); related publication, Kokubu, M., Kobayashi, M., Okamura, H. and Yamamoto, Y. (1975). "Problems of lightweight aggregate concrete." *Selected papers of Masatane Kokubu Studies on Materials for Concrete Structures*, 315-343.

Maekawa, K., Chaube, R. and Kishi, T. (1999). "*Modeling of Concrete Performance.*" London, E & FN Spon.

Maekawa, K., Pimanmas, A. and Okamura, H. (2003). "*Nonlinear Mechanics of Reinforced Concrete.*" London, Spon Press, 2003.

Maekawa, K., Ishida, T. and Kishi, T. (2003). "Multi-scale modeling of concrete performance — Integrated material and structural mechanics." *Journal*

of Advanced Concrete Technology, 1(2), 91-126.

Nakarai, K. and Ishida, T. (2003). "Modeling of Time-dependent Material Properties of Cemented Soil based on Thermodynamic Approach." *The Ninth East Asia-Pacific Conference on Structural Engineering and Construction (EASEC-9)*.

Neville, A. M. (1970). "*Creep of Concrete.*" Amsterdam: North-Holland Publishing Co.

Neville, A. M. (1995). "*Properties of Concrete, Fourth Edition.*" New York: John Wiley & Sons.

Okamura, H. (2000). "*Engineering of Reinforced Concrete.*" Ichigaya Publishing Co., Ltd.,16. (in Japanese)

Ono, H. and Shimomura, T. (2005). "Role of aggregate in shrinkage of concrete." *Proceedings of Japan Concrete Institute*, 27(1), 457-462. (in Japanese)

Snowdon, L. and Edwards, A. (1962). "The moisture movement of natural aggregate and its effect on concrete." *Magazine of Concrete Research*, 14(41), 109-116.

Tatematsu, K., Arai, M., Iwashimizu, T., Kimura, Y., Urano, H., Imamoto, K. and Motoki, R. (2001). "Experimental study on drying shrinkage and pore size distribution of aggregate in Kansai area." *Journal of Structural and Construction Engineering*, Architectural Institute of Japan, No.549, 1-6. (in Japanese)

Tazawa, E., Miyazawa, S., Sato, T. and Konishi, K. (1992). "Autogenous shrinkage of concrete." *Proceedings of the Japan Concrete Institute*, 14(1), 561-566. (in Japanese)

Troxell, G. E., Raphael, J. E. and Davis, R. W. (1958). "Long-time creep and shrinkage tests of plain and reinforced concrete." *Proceeding of ASTM*, 58, 1101-1120.

Upendra, J. C. (1964). "The effect of the elastic modulus of the aggregate on the elastic modulus, creep and creep recovery of concrete." *Magazine of Concrete Research*, 16(48), 129-138.

Zhu, Y., Ishida, T. and Maekawa, K. (2004). "Multi-scale constitutive model of concrete based on thermodynamic states of moisture in micro-pores." *Proceedings of JSCE*, 760(V-63), 241-260. (in Japanese)